Control of transients in drinking water networks

A. Martin [a], J.A. Delgado-Aguiñaga [b,*], V. Puig [a]

[a] Institut de Robòtica i Informàtica Industrial, CSIC-UPC, Llorens i Artigas 4-6, 08028 Barcelona, Spain
[b] Centro de Investigación, Innovación y Desarrollo Tecnológico CIIDETEC-UVM, Universidad del Valle de México, Campus Guadalajara Sur, CP 45601 Tlaquepaque, Jalisco, Mexico

Keywords:
Water distribution systems
Finite-difference approximation
Hydraulic transients
Model predictive control

A B S T R A C T

In this paper, we propose a model-based design approach for the effective control of a drinking water system to reduce the effect of hydraulic transients and meet pressure service requirements regardless of the demand pattern. We model pressure drops along a drinking water system according to a finite-difference approximation of the classical water hammer equations (WHE), and then apply the proposed control strategy to a section of the distribution network located in the metropolitan city of Barcelona. First, a model of the case study network is derived to reproduce the sustained pressure oscillations measured in the real system. Second, a decentralized control scheme composed of an optimal proportional–integrative (PI) controller with anti-windup and a series of model predictive controllers are designed. This control architecture allows to optimally regulate the service pressure while satisfying safety constraints, regardless of water demand fluctuations. Numerical simulations are used to assess the effectiveness of the proposed solution.

1. Introduction

The management and control of a water distribution system ensures pressure regulation and minimizes the risk of water shortages, nonetheless, there are other operational objectives such as minimizing electricity costs due to pump and valve actuation and avoiding dangerous overpressures, among others, which require considerable attention. To achieve these objectives, water distribution networks (WDNs) are usually split into homogeneous areas known as district metered areas (DMAs) that are controlled in a hierarchical fashion (Walski, et al., 2003). High-level optimal controllers compute the pressure set-point for each DMA based on an economic cost–benefit analysis performed over the entire supply network, whereas low-level controllers are used to drive the service pressure to the desired reference. The design of low-level controllers for pressure reducing valves (PRVs) plays a fundamental role in the safekeeping of water distribution networks, enabling a resource-efficient operation, a reduction of background leakage and a lower incidence of pipe bursts. Unfortunately, most of the control solutions proposed in the scientific literature do not focus on the joint dynamics of the controller and the system model (Janus & Ulanicki, 2018). Similarly, most water utilities rely on simple steady-state models for the design, supervision and control. In fact, only in the last few years the scientific community has focused on understanding the dynamic behavior of combined valve-network systems through the impact of hydraulic transients.

Modulating valves were incorporated into a transient simulation software in McInnis, Karney, and Axworthy (1997), while the effect of their automatic operation on transient dynamics was first analyzed in Brunone and Morelli (1999) as a pioneering work. The authors showed a correlation between water flow and pressure oscillations with higher amplitudes under low flow conditions, and they also introduced a novel technique to evaluate the flow-rate curve of a valve through unsteady-state tests. In Bergant, Vitkovsky, Simpson, and Lambert (2001), authors investigated the effects of slow and rapid valve closures on the transient response and compared the data measured using a laboratory apparatus and a hydroelectric power plant with those provided by the simulation model proposed in Brunone and Morelli (1999). Starting with the physical operation principle, two phenomenological models for PRVs are derived in Prescott and Ulanicki (2003). The authors further present a lower-complexity behavioral model and a linear model, where the latter is obtained neglecting the needle valve setting that controls the valve speed. The effects of installing multiple PRVs within the same water distribution system were studied in Prescott and Ulanicki (2004), while the application of a proportional–integral–derivative (PID) control scheme to a theoretical DMA with a single input was proposed in Prescott, Ulanicki, and Renshaw (2005). Driven by the experimental observation of the undesirable phenomena – such as sustained or slowly decaying oscillation or large pressure overshoot – the same authors expanded their previous work to multi-input DMAs to investigate the interaction between valves in Prescott and Ulanicki (2008). Particularly, unsteady-flow network models with random pulsed demands were combined with a behavioral valve model and used to numerically analyze the feedback control

* Corresponding author.
E-mail address: jorge.delgado@uvmnet.edu (J.A. Delgado-Aguiñaga).

of PRVs in very small time steps in the order of milliseconds. As a result, the authors proposed a PID control mechanism tuned with the Åström's relay method (Amstrom & Hagglund, 1995) to improve the network response time with respect to the existing hydraulically-controlled PRVs. In AbdelMeguid, Skworcow, and Ulanicki (2011), the authors developed the controller AQUAI-MOD® aimed at modulating the local control valve outlet pressure according to the real-time measurements of the flow through the valve itself. Notably, the authors demonstrated that a locally controlled valve enables larger service pressure abatement in the water distribution network with beneficial effects in terms of leakage reduction. A more formal stability analysis was first conducted in Ulanicki and Skworcow (2014). In this work, the oscillations recorded under very low flow conditions in a real plant and controlled by an electronically-controlled PRV running a PID algorithm, were successfully reproduced in simulation. The cause of instability was found in the non-linearity of the water system gain, which changes significantly with the opening of the control valve. Furthermore, it was excluded that instability can arise from events in the hydraulic systems – such as pipe bursts – provided that the control system is properly designed. Simultaneously, the pressure waves produced during partial closures and openings of a valve were measured and analyzed using a wavelet transform in Meniconi, et al. (2015). Further experimental studies intended to characterize the dynamic response of PRVs under different flow conditions were presented in Meniconi, Brunone, Mazzetti, Laucelli, and Borta (2016, 2017). More recently, an unsteady-flow model was exploited in Creaco, Campisano, and Modica (2018) to numerically analyze the behavior of remotely controlled valves during challenging hydrant activation scenarios for firefighting. Due to the sensing potential of the pressure signal from remote critical nodes, real-time control schemes were proven to improve service pressure regulation by avoiding pressure deficits that may occur in the presence of static PRVs. An instability event recorded in a large-scale pressure control scheme in one of the major cities in the United Kingdom brought the stability issue back to the table. In Janus and Ulanicki (2018), the authors showed that the loss of stability was a direct consequence of the increase in the static valve-network gain. Indeed, this makes pressure changes more sensitive to valve position adjustments as the valve position gets smaller. In order to tackle the occurrence of instabilities, a nonlinear gain compensator was successfully implemented inside the PID control loop. In Galuppini, Creaco, Toffanin, and Magni (2019), the benefits of considering the dynamic behavior of the hydraulic network in the setup of real-time control algorithms working at a higher sampling rate were investigated, and a filtered PI controller and a linear–quadratic-Gaussian (LQG) model-based controller were proposed. **State-of-the-art techniques for real time control of WDNs are described in** Creaco, et al. (2019).

This work is motivated by an industrial case study proposed by the water company *Aigües de Barcelona*, and it aims to remedy the generation of sustained pressure oscillations caused by the operation of the currently adopted automatic control system. The main contributions of this paper are: (1) the construction of a dynamic hydraulic simulator for a complex, multi-input, real-life network that is able to reproduce the transients produced by the valve opening/closing, (2) the LMI design of an optimal PI controller for the valves that includes a mechanism to cope with the nonlinear behavior, and (3) the design of a predictive control scheme to guarantee optimal safe trajectory tracking of the DMA service pressure with several valves presenting interaction. To describe the dynamic behavior of the case study network, we first present a finite-difference approximation of the continuity and momentum equations that govern transient flows in pressurized closed conduits. Next, we extend the classical formulation to compute pressure drops according to the Hazen–Williams formula and quantify the impact of branching junctions, partial pipeline blockages and dynamically coupled PRVs.

The remainder of the paper is organized as follows. The case study is described in Section 2. The construction of the hydraulic simulator, starting from the mathematical modeling of transient events, is detailed in Section 3. Section 4 describes the different stages of the control system design, whereas the effectiveness of the proposed solution is assessed in Section 5. Finally, in Section 6, the main conclusions are drawn, and future research directions are highlighted.

2. Case study

This paper considers the case study of a section of the Barcelona drinking water network, which corresponds to the pressure zone at a 55 m height of the water column. This part of the network is composed of a main pipeline that conveys water from the upstream fixed-head reservoir down to five different DMAs, arranged one after another as schematically shown in Fig. 1.

The first DMA is supplied through a single PRV, while the remaining ones leverage a multi-feed scheme. Each valve runs an independent hysteresis control algorithm to regulate the service pressure at the entrance of each DMA. Moreover, an additional control valve, denoted as header valve, is placed right after the reservoir to limit the maximum hydraulic head along the main pipe. The physical and topological properties of the case study network are collected using the EPANET hydraulic model depicted in Fig. 2a, kindly provided by the water company *Aigües de Barcelona*.

The EPANET representation features 12203 junctions and 12646 pipes, thus making the thorough modeling and simulation of its dynamic behavior prohibitive. Nevertheless, the availability of flow meter readings at the entrance of each DMA allows to concentrate the water demand of each sector into a single node. To avoid losing consistency, the water demand needs to be treated as a time-varying boundary condition. In light of this observation, the network graph can be pruned right after the PRVs and the accurate description of the DMA subnetworks can be bypassed. In this way, the tractable model shown in Fig. 2b is obtained, where the main pipeline of the network is clearly highlighted. In this simplified hydraulic model, however, the control valves pertaining to the same DMA appear as if they were independent terminals. In order to correctly account for the strong dynamical coupling between the service pressure regulated by such actuators, their downstream nodes have been connected together on a fictitious junction. The length and diameter of the virtual links have been computed according to the equivalent pipe method.

The transient phenomenon that drew the attention of the water company *Aigües de Barcelona* and that motivated the development of this work is shown in Fig. 3.

At night, in response to the reduction of the water demand (drawn with a blue line in the image), sustained oscillations in the valve downstream pressure are observed. The records of the data logger show that these waves propagate throughout the whole pipeline system before they spontaneously decay early in the morning as the water demand and flow through the PRV increase.

3. Transient modeling

3.1. Modeling principles

Hydraulic transient models are developed based on the conservation rules of mass and momentum that characterize transient flows in closed conduits. An unsteady flow in pressurized pipes is governed by a set of one-dimensional quasi-linear-hyperbolic partial differential equations (PDEs), since flow velocity and pressure are functions of both time t and distance x. These equations are derived under the following assumptions: the pipeline is straight without any fitting or slope, the fluid is slightly compressible, the duct wall is slightly deformable, and the convective velocity changes are negligible; likewise, the pipeline cross-section area and fluid density are constant. Then, the PDEs governing the fluid transient response can be written as (Chaudhry, 2014):

Fig. 1. Schematic representation of the homogeneous pressure area.

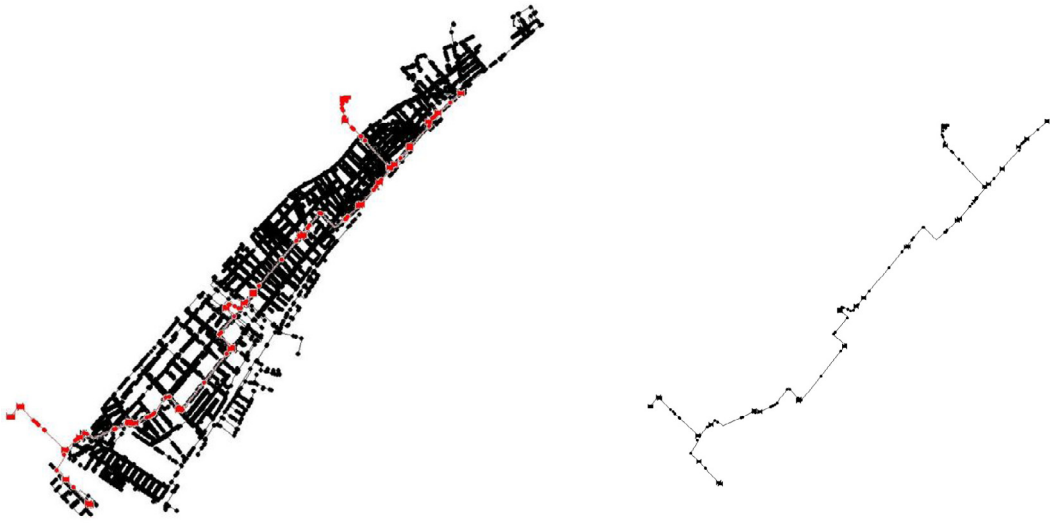

(a) *Original hydraulic model.* (b) *Simplified hydraulic model.*

Fig. 2. EPANET representation of the homogeneous pressure area under study.

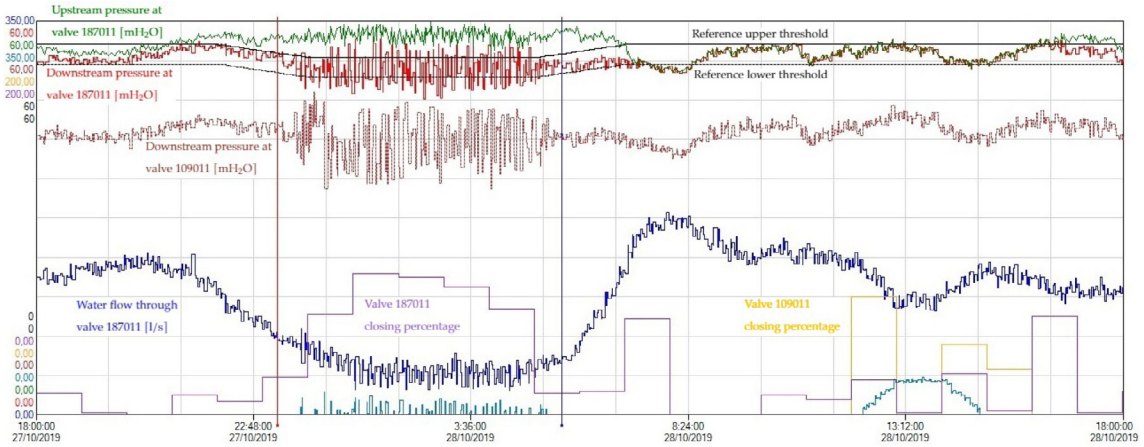

Fig. 3. Sustained oscillations in the valve downstream pressure recorded in the water distribution network during the day-to-night setpoint transition (courtesy of *Aigües de Barcelona*). (For interpretation of the references to color in this figure legend, the reader is referred to the web version of this article.)

Momentum Equation

$$\frac{\partial Q(x,t)}{\partial t} + gA\frac{\partial H(x,t)}{\partial x} + \mu Q(x,t)\,|Q(x,t)| = 0\,, \tag{1}$$

Continuity Equation

$$\frac{\partial H(x,t)}{\partial t} + \frac{b^2}{gA}\frac{\partial Q(x,t)}{\partial x} = 0\,, \tag{2}$$

where Q is the flow rate $[m^3/s]$, H is the pressure head $[m]$, x the length coordinate $[m]$, t the time coordinate $[s]$, g the gravity acceleration $[m/s^2]$, A the cross-section area $[m^2]$, b the pressure wave speed in the fluid $[m/s]$, $\mu = f(Q)/2\phi A$, with ϕ the inner diameter $[m]$ and f the friction factor.

Here, $x \in [0, L]$ denotes the position along the pipe, and L is the equivalent straight length, Mataix (1986).

A closed-form solution of governing Eqs. (1) and (2) is not available in general and is only known for some specific boundary conditions. Here, a solution based on a finite-difference scheme is used. Thus, the

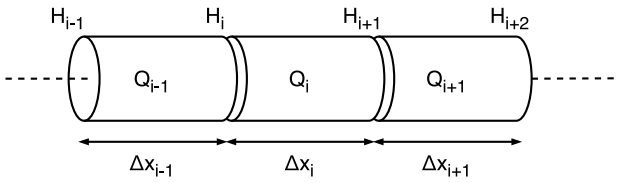

Fig. 4. Finite-difference approximation for pipeline dynamics.

Table 1
Flow dynamics approximation for different boundary conditions.

Boundary conditions	Finite-difference approximation
$[H_{in}\ H_{out}]$	$\dot{Q}_i = \frac{-gA}{\Delta x_i}(H_{i+1} - H_i) - \mu_i Q_i\lvert Q_i\rvert \quad \forall i = 1,\dots,n$ $\dot{H}_{i+1} = \frac{-b^2}{gA\Delta x_i}(Q_{i+1} - Q_i) \quad \forall i = 1,\dots,n-1$
$[Q_{in}\ H_{out}]$	$\dot{Q}_{i+1} = \frac{-gA}{\Delta x_i}(H_{i+1} - H_i) - \mu_{i+1} Q_{i+1}\lvert Q_{i+1}\rvert \quad \forall i = 1,\dots,n$ $\dot{H}_i = \frac{-b^2}{gA\Delta x_{i-1}}(Q_{i+1} - Q_i) \quad \forall i = 1,\dots,n-1;\ \Delta x_0 = 1$
$[H_{in}\ Q_{out}]$	$\dot{Q}_i = \frac{-gA}{\Delta x_i}(H_{i+1} - H_i) - \mu_i Q_i\lvert Q_i\rvert \quad \forall i = 1,\dots,n-1$ $\dot{H}_{i+1} = \frac{-b^2}{gA\Delta x_i}(Q_{i+1} - Q_i) \quad \forall i = 1,\dots,n$
$[Q_{in}\ Q_{out}]$	$\dot{Q}_{i+1} = \frac{-gA}{\Delta x_i}(H_{i+1} - H_i) - \mu_i Q_{i+1}\lvert Q_{i+1}\rvert \quad \forall i = 1,\dots,n$ $\dot{H}_i = \frac{-b^2}{gA\Delta x_{i-1}}(Q_{i+1} - Q_i) \quad \forall i = 1,\dots,n$

partial derivatives are approximated as follows (Chaudhry, 2014):

$$\frac{\partial Q(x_i,t)}{\partial x} \approx \frac{\Delta Q_i}{\Delta x_i} = \frac{Q_i - Q_{i-1}}{x_{i+1} - x_i} \quad \text{and} \quad \frac{\partial H(x_i,t)}{\partial x} \approx \frac{\Delta H_i}{\Delta x_i} = \frac{H_{i+1} - H_i}{x_{i+1} - x_i}, \tag{3}$$

where x_i, H_i and Q_i, $i \in \{1 \dots n\}$ denote the position along the pipe, pressure and outflow at that point, respectively. **This finite-difference approximation is stable if**

$$\Delta x \geq b\Delta t, \tag{4}$$

as per the *Courant–Friedrich–Lewy* stability condition (Chaudhry, 2014). The considered finite-difference-based pipeline dynamics can be appreciated graphically in Fig. 4.

Four different finite-difference approximations of the flow dynamics can be obtained, depending on the choice of boundary conditions. These approximations are compactly presented in Table 1, where $\mu_i = f(Q_i)/2\phi A$.

The model of $f(Q)$ depends on the range of Re and the values of ε encountered in each particular application (Genić, et al., 2011). Namely, a model of $f(Q_i)$ can be chosen as:

$$f(Q_i) = \frac{0.25}{\left[log_{10}\left(\frac{\varepsilon}{3.7\phi} + \frac{5.74}{Re(Q_i)^{0.9}}\right)\right]^2}, \tag{5}$$

where $\varepsilon \in [1 \times 10^{-6},\ 0.05]$ is the roughness of the pipe in $[m]$ and $Re \in [5000,\ 10^8]$ is the Reynolds number [dimensionless]. The latter is given by $Re(Q_i) = Q_i\phi/\nu A_r$, where ν is the kinematic viscosity of water in $[m^2/s]$, which can be calculated as in Delgado-Aguiñaga, Begovich, and Besançon (2016).

In our case study, the boundary conditions are the fixed reservoir elevation at the upstream end of the network and water outflow at its downstream end, which we set equal to the time-varying user demand. Proceeding as detailed in Table 1 and by rearranging terms, the set of nonlinear ordinary differential equations are

$$\begin{aligned} \dot{H}_{i+1} &= -\frac{-b^2}{gA}\frac{Q_{i+1} - Q_i}{x_{i+1} - x_i} \quad \forall i = 1,\dots,n-1, \\ \dot{Q}_i &= -Ag\frac{H_{i+1} - H_i}{x_{i+1} - x_i} - \frac{f_i Q_i\lvert Q_i\rvert}{2\phi A} \quad \forall i = 1,\dots,n, \end{aligned} \tag{6}$$

with the boundary conditions $H_1 = H_{in}$ and $Q_n = Q_{out}$.

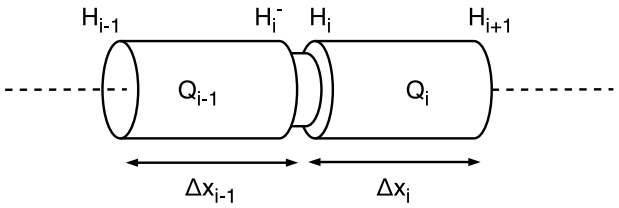

Fig. 5. Partial pipeline blockage at position x_i.

On the other hand, interconnecting single elements as pipes, valves and reservoirs, among others, complex pipeline configurations, including loops and branches can be formed. To correctly handle a complex pipeline system, we need to consider a couple of special boundary conditions in addition to the previous ones, namely (i) series junctions and (ii) branch connections. These will allow us to develop a solution procedure for such complex systems (Wylie, Streeter, & Suo, 1993). The continuity equation describing the mass conservation at a junction may be written as

$$\sum_{i=1}^{P_k} Q_i + Q_{out} = 0, \tag{7}$$

where Q_i represents the flow in a pipe i, Q_{out} is any inflow or outflow, and P_k is the number of pipes at the junction. Inflows are considered positive and outflows are considered negative. Moreover, since there is no storage capacity at any junction, a common head is assumed when minor effects are neglected (Wylie et al., 1993).

In practice, water management companies usually employ the well-known Hazen–Williams equation to compute the head-losses (Dini & Tabesh, 2014; Kara, Karadirek, Muhammetoglu, & Muhammetoglu, 2016):

$$\Delta H = 10.65\frac{Q^{1.85}}{C^{1.85}}\frac{L}{\phi^{4.87}}, \tag{8}$$

where ΔH is the head loss through a pipeline of length L, Q is the flow rate $[m^3/s]$, ϕ is the inner diameter $[m]$, and C is the Hazen William's coefficient.

Next, we also consider and model changes in the diameter of two consecutive pipeline sections. This reduction can be seen as a partial blockage at position x_i, see Fig. 5. An appropriate modeling considering such an effect can be described as follows (Besançon, Guillén, Dulhoste, Santos, & Scola, 2013):

$$\begin{aligned} \dot{H}_{i-1} &= \frac{-b^2}{gA_r}\frac{(Q_{i-1} - Q_{i-2})}{x_i - x_{i-1}}, \\ \dot{Q}_{i-1} &= -gA_r\frac{(H_i^- - H_{i-1})}{x_i - x_{i-1}} - \mu_{i-1}Q_{i-1}\lvert Q_{i-1}\rvert, \\ \dot{H}_i &= \frac{-b^2}{gA_r}\frac{(Q_i - Q_{i-1})}{x_{i+1} - x_i}, \\ \dot{Q}_i &= -gA_r\frac{(H_{i+1} - H_i)}{x_{i+1} - x_i} - \mu_i Q_i\lvert Q_i\rvert, \end{aligned} \tag{9}$$

where H_i^- denotes the pressure just before the blockage. The application of Bernoulli's equation between the position just before the blockage x_i^- and the position x_i yields

$$H_i^- = H_i - \frac{Q_{i-1}^2}{2g(A_i^-)^2}\left[1 - \left(\frac{A_i^-}{A_i}\right)^2\right], \tag{10}$$

which can be introduced in (9). Here, we denote with A_i the constant transversal section area, which is reduced only at $x = x_i$.

3.2. Validation of the hydraulic simulator

An hydraulic simulator resembling the dynamic behavior of the case study network has been constructed in MATALB/Simulink using the

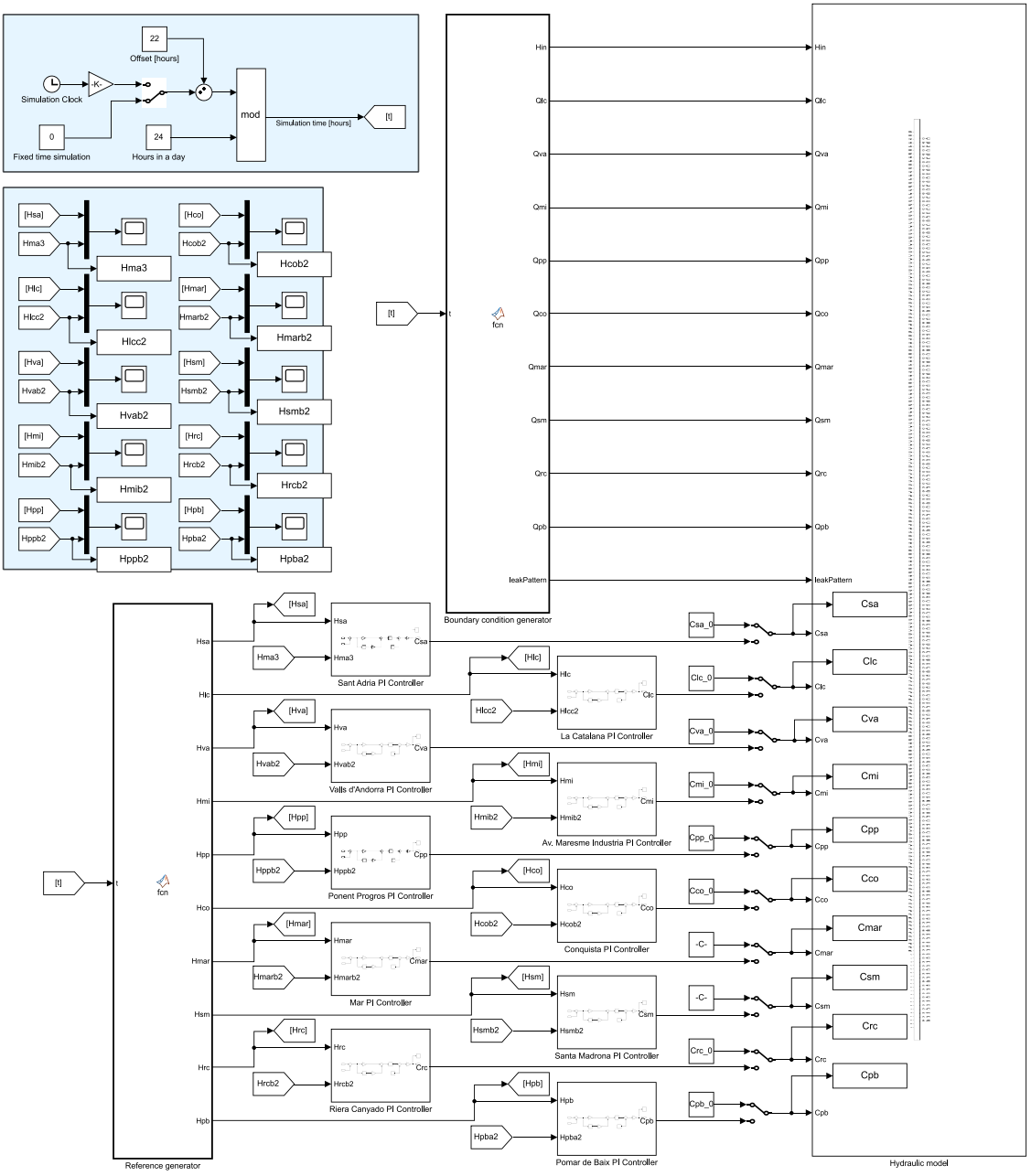

Fig. 6. Overview of the hydraulic simulator as Simulink block diagram model.

finite-difference approximation (6) of the unsteady-flow equations. The schematic diagram of the simulator is shown in Fig. 6.

To simulate the dynamic behavior with respect to the simplified EPANET representation presented in Fig. 2b, the considered drinking water system has been subdivided into a series of homogeneous pipeline sections, starting from the reservoir located at the upstream end, and following the direction of the water flow. Next, for each node, the pressure and discharge time derivatives have been computed. In doing so, we have taken into account the eventual presence of partial pipeline blockages, branching junctions or PRVs, and the physical parameters of the section, such as elevation of the extreme nodes, pipe diameter, length, and roughness. Auxiliary blocks are further used to set a proper initial condition for the system, and generate according to the elapsed simulation time, the time-varying water demand of each DMA. Similarly, these blocks account for the computation of the downstream pressure references that the control valves should track. In particular, the pressure head at the upstream end of the pipeline system is kept constant and the daily evolution of the network downstream boundary conditions is obtained by the linear interpolation of the water demand measurements available from the real system.

A few comments about the validation of the developed hydraulic simulator are described next. First, the evolution of the Reynolds number for the flow in the main pipeline over a whole day, shown in Fig. 7, backs up the usage of the Hazen–Williams formula for the computation of the pressure head losses due to friction.

In fact, since the Reynolds number is significantly higher than 4000, the upper threshold for the flow lies within the critical region, and thus a turbulent flow regime can be assumed. Second, the developed hydraulic simulator represents at least the steady-state behavior of the actual network and its predictions are aligned with those of the EPANET model, which is accepted by the water company *Aigües de Barcelona*. As an example, Fig. 8 shows that initializing the system in a steady state calculated with EPANET (dotted lines), the equilibrium configuration is maintained in the proposed simulator until an event

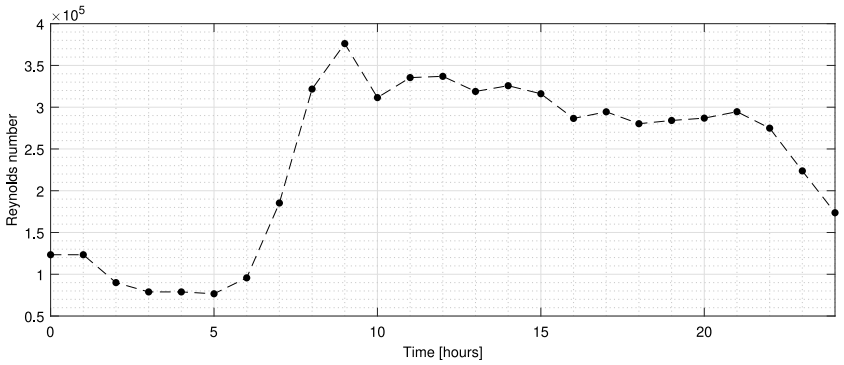

Fig. 7. Daily evolution of the Reynolds number at the upstream end of the main pipeline.

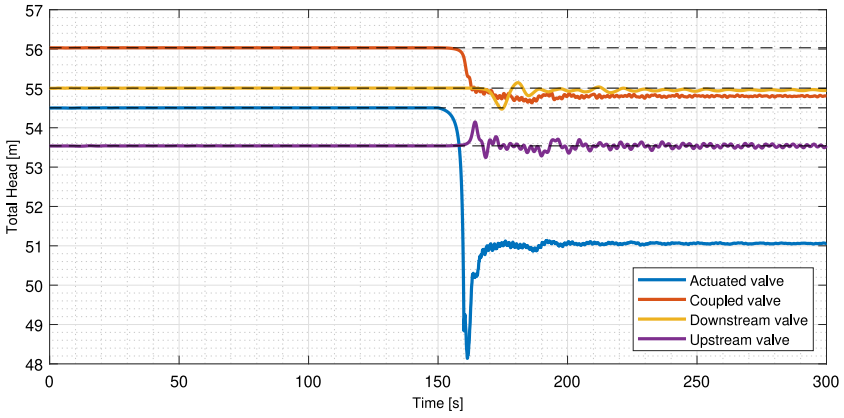

Fig. 8. Partial valve closure effect on the pressure head in different nodes of the network.

occurs, namely until a sudden partial close of the control valve occurs. **Considering the available instruments in the real case study network, it was not possible to fully validate the simulation of hydraulic transients. However, the proposed modeling methodology has been successfully implemented and validated to reproduce transients on a smaller real case study in** Delgado-Aguiñaga and Begovich (2017) **by only adjusting the steady state behavior.** Finally, in regard to the same figure, the effect of the partial closure of a control valve on the service pressure (at the entrance of the remaining DMAs) is correctly sensed. The effect also shows a time delay that increases with the physical distance dividing the two sectors. This phenomenon, attributable to the finite sonic velocity of the pressure waves, has also been pointed out in Galuppini, Magni, and Creaco (2020). Fig. 8 further illustrates the potential of the proposed simulator as it shows the significant negative peak in the service pressure provoked by a sudden partial valve closure as well as the effect of such change on the service pressure at different nodes of the network. Note that small and decaying oscillations are registered in the service pressure of the upstream sectors, with almost no variation in their steady-state value. On the other hand, since a multi-feed scheme is adopted, the partial closure of a control valve implies a redistribution of the total water demand of the DMA across its valves. In turn, for the mass conservation rule, this adjustment forces a change in the discharge of the main pipeline section connecting such valves. Consequently, an effect from operating the control valve is propagated and the steady-state value of the service pressure in the downstream sectors may vary.

4. Control system design

The nonlinear simulation model, which has been constructed starting from the mass and momentum conservation rules, is not suitable for the design of a control scheme that includes online optimization algorithms, due to its high complexity. Therefore, we relied on simpler control-oriented models for the controller synthesis. These models only describe the response of the most relevant hydraulic variables, including actuation commands and external disturbances. Our first efforts focused towards obtaining a global mathematical representation of the water network's behavior in the form of a transfer function matrix. In other words, we initially searched for a relationship between the opening percentage of each valve and the regulated vector of downstream pressures to explain the numerical data obtained in simulation. However, due to the difficulties associated with isolating the effect of the operation in a single control valve, this approach has not been deepened in favor of a local system description. Indeed, such effect is nonlinear, and it highly depends on the network's working point. The resulting decentralized control scheme treats the header and sector valves independently and only accounts for the dynamical coupling between valves of the same DMA.

4.1. Header valve control

The header valve is directly connected to the fixed head reservoir. Consequently, its upstream pressure level only presents small variations during the day. Indeed, the head losses generated along the main pipe vary as the total water demand of the case study network changes. Moreover, its downstream pressure is not significantly affected by the operation of the sector valves since the pressure waves barely back-propagate against the direction of the water flow and up to the initial node of the network. The reference signal also exhibits smooth rather than sharp transitions. For these reasons, an optimal PI controller is proposed.

Since we opted for a local control architecture, since the objective variable is the pressure at the actuator site, a more favorable control

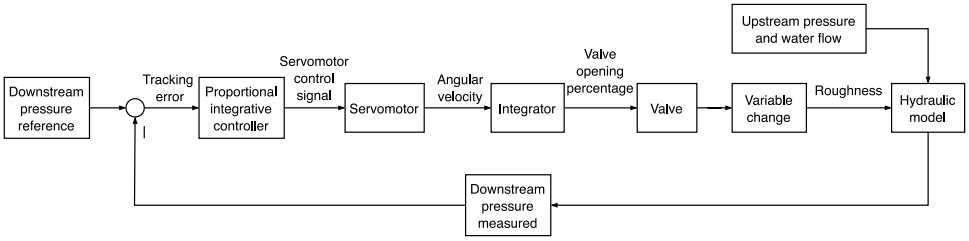

Fig. 9. Block diagram representation of the control scheme for the header valve.

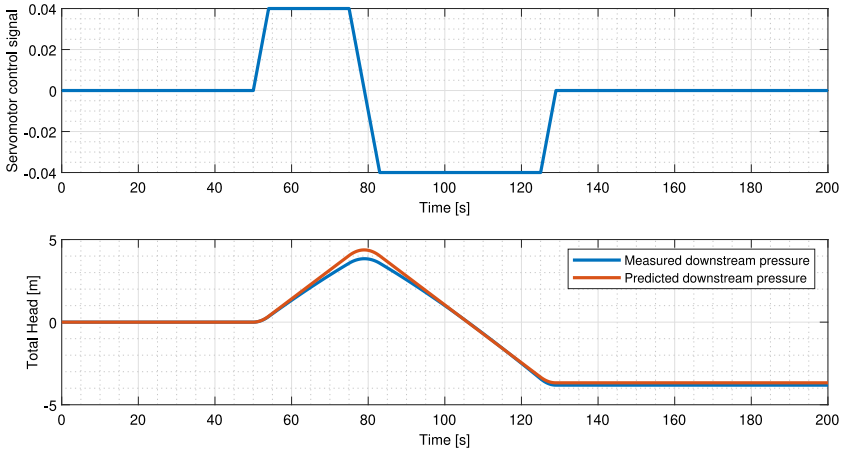

Fig. 10. Identification of the dynamic behavior of the header valve around a working point.

variable is defined through the Hazen–Williams Eq. (8) as follows

$$H = \underbrace{\frac{C^{1.852}\phi^{4.8704}H^{-} - 10.67LQ^{1.852}}{C^{1.852}}}_{C' = \rho(C)} \frac{1}{\phi^{4.8704}}, \tag{11}$$

where we denote with H^{-} the upstream pressure at the control actuator. The advantages of parametrizing the opening percentage of the valve, and in turn, the pressure drop across it, are twofold in terms of this new variable. First, the nonlinear and operating-point-dependent relationship between the Hazen–Williams coefficient C and valve downstream pressure is bypassed. Second, the identification of a control-oriented model is favored.

The block diagram scheme depicted in Fig. 9 is used to identify the state-space model, which describes the dynamic relationship between the servomotor voltage control signal – that regulates the angular velocity at which the valve can be progressively opened or closed – and the consequent variation of the downstream pressure.

Note that the change of variable previously introduced is operated right after the blocks that account for the mechanical structure of the valve. Despite this positioning can be used without any drawback in simulation, a practical implementation of this solution would require placing the linearization block, opportunely re-scaled, just before the servomotor since the latter constitutes the physical medium through which the roughness of the valve is changed. Nevertheless, we point out that while the dynamics of the valve's mechanical structure has been considered for completeness, a major interest lies in the dynamics that originates from the relationships between hydraulic variables. Fig. 9 highlights the presence of a pure integrator in the forward loop between the servomotor control signal and the downstream pressure. In order to account for this information and to impose the observability canonical form[1] to the state-space model $\Sigma_h = (A_h, B_h, C_h, 0)$, the identification has been carried out by optimizing the squared distance between the measured and estimated downstream pressure over the vector of unknown parameters that characterize the matrices of the to-be-identified system. The results obtained on the dataset generated with a sampling time $T_s = 0.1$s using the hydraulic simulator based on the finite-difference approximation of the continuity and momentum equations are shown in Fig. 10.

The dynamic behavior of the header valve is approximated by the linear time-invariant discrete-time model:

$$\begin{aligned} \dot{\mathbf{x}}_h(t) &= A_h\mathbf{x}_h(t) + B_h u_h(t) = \begin{bmatrix} 0 & 0 \\ 1 & -211.35 \end{bmatrix} \mathbf{x}_h(t) + \begin{bmatrix} 92.41 \\ 58.90 \end{bmatrix} u_h(t), \\ y_h(t) &= C_h\mathbf{x}_h(t) = \begin{bmatrix} 0 & 1 \end{bmatrix} \mathbf{x}_h(t). \end{aligned} \tag{12}$$

With the identified state-space representation at hand, the controller gain K can be evaluated as the solution of the linear matrix inequalities (LMIs) problem:

$$\begin{aligned} &\min_{P,K} \operatorname{tr}(P) \\ &\text{subject to } \left(A_h + B_hK\right)^{\mathsf{T}} P + P\left(A_h + B_hK\right) \prec -\Omega - K^{\mathsf{T}}RK, \end{aligned} \tag{13}$$

to minimize a quadratic measure of interest $J = \int_0^\infty \mathbf{x}_h^{\mathsf{T}}(t)\Omega\mathbf{x}_h(t) + u_h(t)^{\mathsf{T}}Ru_h(t)$. Here, P is a positive definite matrix, whereas Ω and R are weights matrices that can be selected according to the desired shape of the closed-loop system response. The semi-definite programming problem (13) is non-convex. Nevertheless, performing a congruence transformation with $Y = P^{-1}$, introducing $L = KY$ and applying a Schur complement yields the equivalent tractable formulation:

$$\begin{aligned} &\max_{Y,L} \operatorname{tr}(P) \\ &\text{subject to } \begin{pmatrix} -\left(A_hY + B_hL\right)^{\mathsf{T}} - \left(A_hY + B_hL\right) & Y & L^{\mathsf{T}} \\ Y & \Omega^{-1} & 0 \\ L & 0 & R^{-1} \end{pmatrix} \succ 0. \end{aligned} \tag{14}$$

The feasibility of these convex constraints has been checked using MATLAB through Yalmip on a standard laptop computer. We let:

$$\Omega = \begin{bmatrix} 0.2 & 0 \\ 0 & 20 \end{bmatrix} \text{ and } R = 1, \tag{15}$$

[1] This choice allows to consider the resulting state-feedback controller as a PI since the state components can be interpreted as the tracking error and its integral.

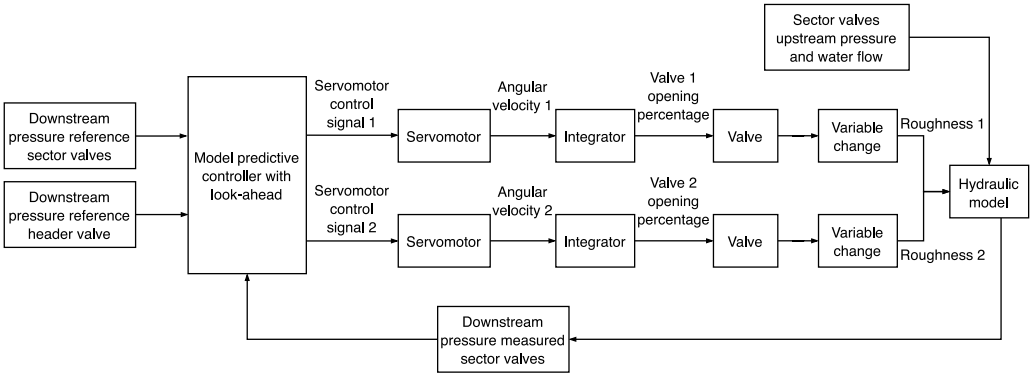

Fig. 11. Block diagram representation of the control scheme for the sector valves.

in order to penalize deviations in the second state component, namely the tracking error with respect to the valve's downstream pressure reference. With this choice, the positive-definite solution

$$Y_f = \begin{bmatrix} 147.126 & 14.501 \\ 14.501 & 27.339 \end{bmatrix}, \tag{16}$$

is obtained. Finally, the controller gain matrix is reconstructed as $K = LY^{-1}$. This yields

$$K = \begin{bmatrix} 0.4389 & 1.9249 \end{bmatrix}. \tag{17}$$

An anti-windup mechanism is further implemented to account for the limited dynamic range of the control valve and improve the control performance in case the latter experiences saturation.

4.2. Sector valve control

Applying the diffeomorphism (11) to each sector valve would yield, in principle, a perfectly decoupled system. In this case, each actuator could be controlled independently simply by compensating in a feed-forward fashion for the variations in its upstream pressure and in the water flow. On the other hand, this solution turns out to be impractical since it is not robust to accurately measure noise and disturbances. Indeed, these environmental issues would be reflected in the actuation commands, leading to nervous valve openings. Moreover, the upstream pressure at the control valves is not measured in the real network. To avoid running into these issues, the simpler transformation

$$\Delta H = H^- - H = \frac{10.67LQ^{1.852}}{C^{1.852}\phi^{4.8704}} = \frac{10.67L}{\phi^{4.8704}} \underbrace{\left(\frac{Q}{C}\right)^{1.852}}_{C' = \psi(C)}, \tag{18}$$

has been considered to define a control parameter that is linear with respect to the pressure drop. With this choice, however, the knowledge of the control variable C' does not completely determine the valve's downstream pressure value. Consequently, an estimation of the upstream pressure will be required in the control design.

The dynamical coupling between control valves that regulate the service pressure at the same DMA is significant. Therefore, we identify a multi-input multi-output system to describe how the actuation commands of each servomotor affect the pressure at the downstream node of each control valve, as illustrated in the block diagram of Fig. 11.

Note that the downstream pressure reference of the header valve has been considered as an additional input to the state-space model to be identified. Notably, this reference is treated as a known disturbance in the design of the predictive controller and it represents an estimation of the upstream pressure at the control valves, which is not sensed. This approximation is backed up by the fact that the considered case study network distinctly presents low flows during the entire day and consequently, low pressure drops along the main pipeline. Next, the system identification toolbox available in MATLAB is used to assess and compare the explanatory capability of several discrete state-space models of different orders. For instance, considering the intermediate DMA labeled as Badalona Port in Fig. 1, we rely on Akaike's final prediction error criterion to select the fourth-order discrete-time state space model $\Sigma_s = (A_s, B_s, C_s, 0)$ defined by the set of equations:

$$\begin{aligned} \mathbf{x}_s(t+1) &= A_s\mathbf{x}_s(t) + B_s\mathbf{u}_s(t) = A_s\mathbf{x}_s(t) + \begin{bmatrix} B_{sd} & B_{su} \end{bmatrix} \begin{bmatrix} d(t) \\ u(t) \end{bmatrix}, \\ y_s(t) &= C_s\mathbf{x}_s(t), \\ A_s &= \begin{bmatrix} -0.389 & 0.780 & 3.982 & 2.666 \\ -0.948 & 1.537 & 2.775 & 2.177 \\ 0.026 & -0.003 & 0.868 & 0.078 \\ 0.017 & -0.016 & -0.041 & 0.851 \end{bmatrix}, \quad B_{sd} = \begin{bmatrix} -2.92 \cdot 10^5 \\ -1.99 \cdot 10^5 \\ 7.86 \cdot 10^3 \\ 2.40 \cdot 10^2 \end{bmatrix}, \\ B_{su} &= \begin{bmatrix} 8.94 \cdot 10^8 & -6.95 \cdot 10^8 \\ 6.11 \cdot 10^8 & -4.76 \cdot 10^8 \\ -2.41 \cdot 10^7 & 1.88 \cdot 10^7 \\ -7.36 \cdot 10^6 & 5.68 \cdot 10^6 \end{bmatrix}, \\ C_s &= \begin{bmatrix} -0.003799 & 0.01354 & 0.1106 & 0.3046 \\ 0.0862 & -0.1327 & -0.09033 & -0.2632 \end{bmatrix}. \end{aligned} \tag{19}$$

Here, u denotes the vector of servomotor control signals, whereas d is the known disturbance that affects the state dynamics through the matrix B_{sd}. As it can be seen in Fig. 12, which shows the graphic interface of the identification toolbox, this model fits the experimental data accurately, although it fails to explain some oscillations recorded in the simulation process. Nevertheless, higher order state-space models did not capture such dynamics. Therefore, a reduced-order model has been selected for the sake of simplicity.

For the purpose of jointly controlling the valves feeding a particular DMA, a model predictive control scheme has been implemented. This choice is motivated by its unique ability to handle an internal dynamic model of the process and management of physical constraints on the system's inputs and outputs while optimizing a performance index. Moreover, this architecture allows to exploit the a priori knowledge of the control valve reference r. In fact, at every time step, the applied control action is obtained by solving online the finite-horizon optimal control problem,

$$\begin{aligned} \min_{u_0 \dots u_N} \; & \frac{1}{2}(r_N - y_N)^\top S(r_N - y_N) \\ & + \frac{1}{2}\left(\sum_{k=0}^{N-1}(r_k - y_k)^\top \Omega(r_k - y_k) + \Delta u_k^\top R \Delta u_k\right) \\ \text{subject to} \; & x_{k+1} = Ax_k + B_u u_k + B_d d_k, \quad y_k = Cx_k, \quad \forall k \in \{0 \dots N\}, \\ & x_0 \text{ known}, \quad u_{min} \le u_k \le u_{max}, \quad \Delta u_{min} \le |u_{k+1} - u_k| \le \Delta u_{max}, \end{aligned} \tag{20}$$

where N represents the prediction horizon. Note that both the objective function and the constraints explicitly depend on the reference and the known disturbances. Precisely, by introducing a preview of both

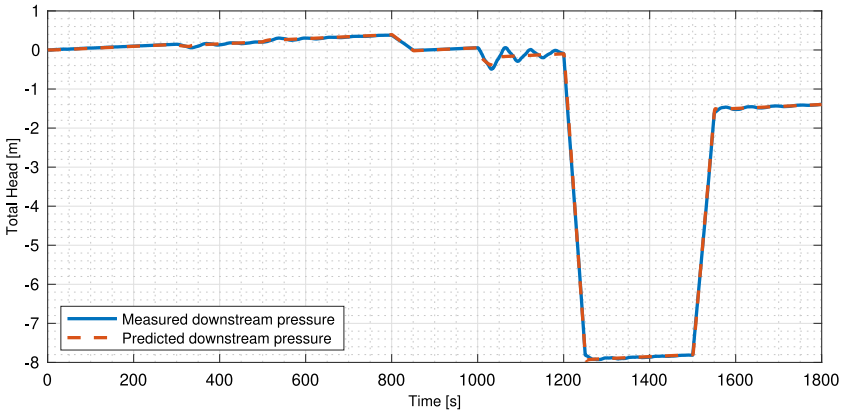

Fig. 12. Identification of the dynamic behavior of the sector valves around a working point.

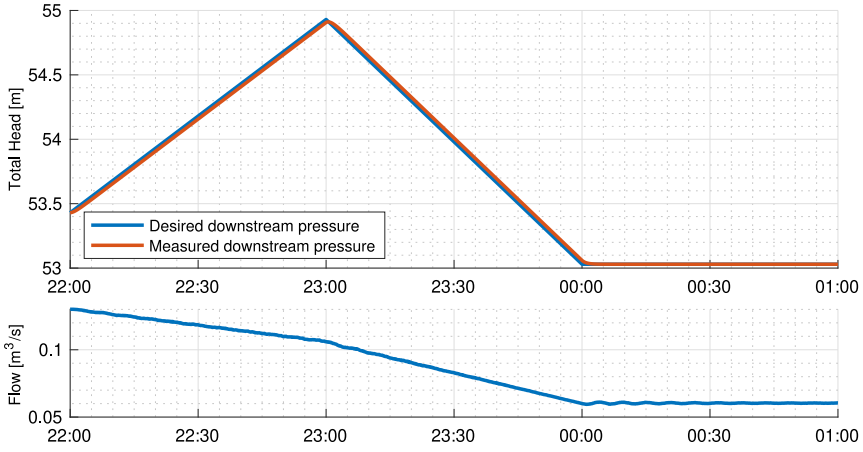

(a) Header valve control.

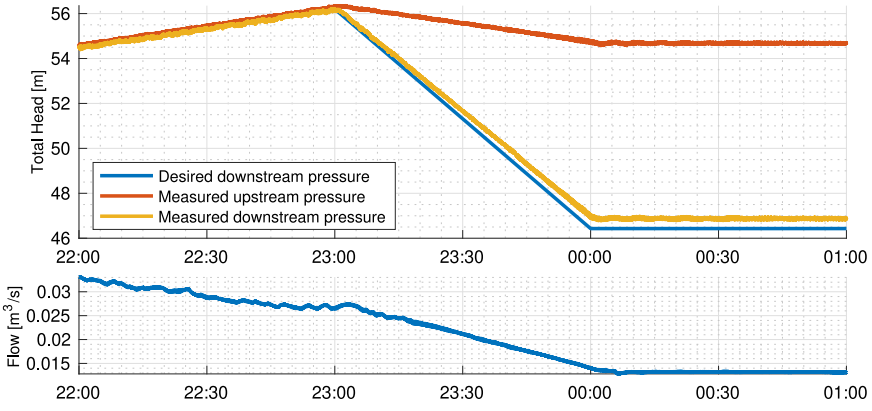

(b) Sector valves control.

Fig. 13. Daily-to-nocturnal pressure set-point transition and the entrance of a DMA.

the disturbance and reference signals, the control performance can be improved by the user. Such improvement is more significant during the transition from the diurnal to the nocturnal pressure reference and vice versa, namely in the time span where sustained pressure waves were recorded in the real system. Since hydraulic networks are fairly slow systems, in the design of the predictive controller we selected a sampling time $T_s = 0.1$ s, a prediction horizon of 50 samples and a control horizon of 20 samples.

5. Results

The effectiveness of the proposed solution has been assessed by performing an extended network simulation over the hydraulic simulator presented in Section 3. Particularly, Fig. 13 collects the results obtained during the daily-to-nocturnal pressure set-point transition for both the header and sector valves. This challenging scenario was proven to generate sustained pressure oscillations in the real system (as shown

in Fig. 3), whereas the proposed control architecture manages to safely and smoothly regulate the system.

On the other hand, Fig. 13(a) shows that the state-feedback controller manages to adjust the header valve to almost perfectly track the downstream pressure reference.

Indeed, the measured downstream almost perfectly tracks its reference, from which it slightly deviates only in correspondence to a change in the slope of the reference. This should be attributed to the finite valve velocity that does not allow instantaneous adjustments. Regarding the service pressure control at the entrance of the different DMAs, instead, the results of an extended simulation capturing the whole transition from the daily to the nocturnal pressure reference are collected in Fig. 13(b). At first, the valve is fully opened and there is almost no pressure drop across the valve, as pointed out by the overlapping of the yellow and orange curves. During the night, instead, the gap between the two widens quickly until the upstream and downstream nodes of the valve present a difference of roughly 8 m in height of the water column. Even in this more challenging scenario, the model predictive controller manages to track the downstream pressure reference, even though the generation of a non-zero steady state error can be highlighted. The cause for this mismatch should probably be sought in the degradation of the representativeness of the identified model as the valve continues to close, thus changing significantly from the operating conditions around which the identification was carried out. Nevertheless, the proposed control scheme succeeded in avoiding the generation of sustained or slowly-decaying oscillations in the pressure signals and at the same time, the steady-state error shown in Fig. 13(b) can also be considered acceptable for practical purposes.

6. Conclusions

In this paper, a finite-difference approximation of the transient-flow equations has been ambitiously applied to represent the dynamic behavior of a large-scale complex water distribution network, proving the feasibility of this approach. An extension of the classical momentum and continuity equations that allows to compute head losses due to friction using the Hazen–Williams formula has been derived, and the steady-state predictions of the simulator have been validated. On the other hand, regarding the design of a control system, the proposed solution effectively models the interaction between control valves and ensures smooth tracking of the reference signals, while rejecting external disturbances in the form of changes in the water demand. Future work may consider applying a finer discretization grid for the approximation of the pipeline dynamics and exploring the benefits of a linear parameter-varying description of the system dynamics that would allow the deployment of a gain-scheduling control scheme.

Declaration of competing interest

The authors declare that they have no known competing financial interests or personal relationships that could have appeared to influence the work reported in this paper.

References

AbdelMeguid, H., Skworcow, P., & Ulanicki, B. (2011). Mathematical modelling of a hydraulic controller for PRV flow modulation. *Journal of Hydroinformatics*, *13*(3), 374–389.

Amstrom, K., & Hagglund, T. (1995). *PID controllers: Theory, design and tuning*. Research Triangle Park, NC: Instrument Society of America.

Bergant, A., Vitkovsky, J., Simpson, A., & Lambert, M. (2001). Valve induced transients influenced by unsteady pipe flow friction. In *Proc of the 10th int meeting of the work group on the behaviour of hydraulic machinery under steady oscillatory conditions*.

Besançon, G., Guillén, M., Dulhoste, J.-F., Santos, R., & Scola, I. R. (2013). Pipeline partial blockage modeling and identification. *IFAC Proceedings Volumes*, *46*(11), 730–735.

Brunone, B., & Morelli, L. (1999). Automatic control valve–induced transients in operative pipe system. *Journal of Hydraulic Engineering*, *125*(5), 534–542.

Chaudhry, M. H. (2014). *Applied hydraulic transients*. Springer-Verlag New York.

Creaco, E., Campisano, A., Fontana, N., Marini, G., Page, P., & Walski, T. (2019). Real time control of water distribution networks: A state-of-the-art review. *Water Research*, *161*, 517–530.

Creaco, E., Campisano, A., & Modica, C. (2018). Testing behavior and effects of PRVs and RTC valves during hydrant activation scenarios. *Urban Water Journal*, *15*(3), 218–226.

Delgado-Aguiñaga, J. A., & Begovich, O. (2017). Water leak diagnosis in pressurized pipelines: a real case study. In C. Verde, & L. Torres (Eds.), *Modeling and monitoring of pipelines and networks* (pp. 235–262). Springer International Publishing.

Delgado-Aguiñaga, J. A., Begovich, O., & Besançon, G. (2016). Exact-differentiation-based leak detection and isolation in a plastic pipeline under temperature variations. *Journal of Process Control*, *42*, 114–124.

Dini, M., & Tabesh, M. (2014). A new method for simultaneous calibration of demand pattern and hazen-williams coefficients in water distribution systems. *Water Resources Management*, *28*(7), 2021–2034.

Galuppini, G., Creaco, E., Toffanin, C., & Magni, L. (2019). Service pressure regulation in water distribution networks. *Control Engineering Practice*, *86*, 70–84.

Galuppini, G., Magni, L., & Creaco, E. (2020). Stability and robustness of real-time pressure control in water distribution systems. *Journal of Hydraulic Engineering*, *146*(4), Article 04020023.

Genić, S., Arandelović, I., Kolendić, P., Jarić, M., Budimir, N., & Genić, V. (2011). A review of explicit approximations of Colebrook's equation. *FME Transactions*, *39*(2), 67–71.

Janus, T., & Ulanicki, B. (2018). Improving stability of electronically controlled pressure-reducing valves through gain compensation. *Journal of Hydraulic Engineering*, *144*(8), Article 04018053.

Kara, S., Karadirek, I. E., Muhammetoglu, A., & Muhammetoglu, H. (2016). Hydraulic modeling of a water distribution network in a tourism area with highly varying characteristics. *Procedia Engineering*, *162*, 521–529.

Mataix, C. (1986). *Mecánica de fluidos y máquinas hidráulicas*. Ed. Del Castillo.

McInnis, D. A., Karney, B. W., & Axworthy, D. H. (1997). Efficient valve representation in fixed-grid characteristics method. *Journal of Hydraulic Engineering*, *123*(8), 709–718.

Meniconi, S., Brunone, B., Ferrante, M., Mazzetti, E., Laucelli, D. B., & Borta, G. (2015). Transient effects of self-adjustment of pressure reducing valves. *Procedia Engineering*, *119*, 1030–1038.

Meniconi, S., Brunone, B., Mazzetti, E., Laucelli, D. B., & Borta, G. (2016). Pressure reducing valve characterization for pipe system management. *Procedia Engineering*, *162*, 455–462.

Meniconi, S., Brunone, B., Mazzetti, E., Laucelli, D. B., & Borta, G. (2017). Hydraulic characterization and transient response of pressure reducing valves: laboratory experiments. *Journal of Hydroinformatics*, *19*(6), 798–810.

Prescott, S. L., & Ulanicki, B. (2003). Dynamic modeling of pressure reducing valves. *Journal of Hydraulic Engineering*, *129*(10), 804–812.

Prescott, S., & Ulanicki, B. (2004). Investigating interaction between pressure reducing valves and transients in water networks. In *Proccedings 49th int. scientific colloquium (vol. 1)* (pp. 49–54).

Prescott, S. L., & Ulanicki, B. (2008). Improved control of pressure reducing valves in water distribution networks. *Journal of Hydraulic Engineering*, *134*(1), 56–65.

Prescott, S., Ulanicki, B., & Renshaw, J. (2005). Dynamic behavior of water networks controlled by pressure reducing valves. In *CCWI2005—Water management for the 21st century (vol. 1)* (pp. 239–244). Centre for Water Systems.

Ulanicki, B., & Skworcow, P. (2014). Why PRVs tends to oscillate at low flows. *Procedia Engineering*, *89*, 378–385.

Walski, T. M., Chase, D. V., Savic, D. A., Grayman, W., Beckwith, S., & Koelle, E. (2003). *Advanced water distribution modeling and management*. Haestad Press.

Wylie, E. B., Streeter, V. L., & Suo, L. (1993). *Fluid transients in systems (vol. 1)*. NJ: Prentice Hall Englewood Cliffs.